14
Reggeon field theory

Reggeons turn out to be similar to particles with varying spins not only in the sense of the 'pole' contribution to the asymptotics, but also in the interaction picture.

We have started with a Regge pole and generated series of *non-enhanced* reggeon diagrams characterized by non-singular particle–reggeon vertices N,
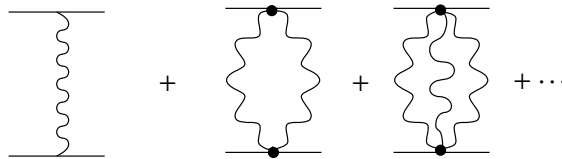
Angular momentum singularities in reggeon creation amplitudes gave rise to various *enhanced* reggeon diagrams,
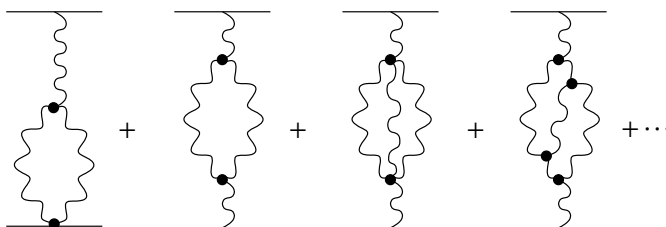
We are looking for an effective field theory that would solve the reggeon unitarity. The usual field theory contains a hypothesis about the form of the interaction. If I chose three-reggeon, or only four-reggeon, interactions

354

to build up the theory,
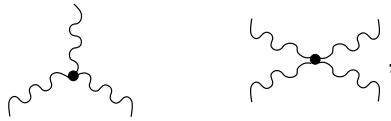
or even employed them together, I would be able to fulfil the corresponding reggeon unitarity conditions. But I have no reason to restrict myself to such vertices. In other words, my 'theory' contains in principle an infinite number of unknown constants.

Everything would have been fine if we had $\alpha(0) < 1$, that is, σ_{tot} decreasing with energy. In this case the branchings are separated from the pole, produce but small controllable corrections to the asymptotics, and the interaction can be looked upon as being weak.

In the interesting case of $\alpha(0) = 1$, however, the multi-reggeon interactions are absolutely essential: at $t = 0$ branchings accumulate to $j = 1$, and for $t < 0$ even move *to the right* from the pomeron pole. This means that from a practical point of view we have lost. From the point of view of the theory, however, the problem, although a complicated one, remains sensible: the iteration of poles and branchings produced but new reggeon branchings, and the picture remained self-consistent.

It is somewhat distressing that the interactions of reggeons cannot be considered as weak ones, so the beauty of reggeons, as objects embodying strong interaction, apparently disappears. Nevertheless, one can hope that in certain cases just a finite number of vertices will be relevant. This being the case, it will allow one to relate different observables and use the reggeon field theory in order to make quantitative as well as qualitative predictions.

14.1 Prescriptions for reggeon diagram technique

To construct a field theory we have to start with the bare propagator and interaction vertices. To describe interacting pomerons it is convenient to introduce the bare **P** Green function as

$$G_0(k) = \frac{-1}{\omega + \varepsilon(\mathbf{k})}\,; \qquad \omega = j - 1, \quad \varepsilon(\mathbf{k}) = -\alpha(k^2) + 1 \simeq \alpha'\mathbf{k}^2. \quad (14.1a)$$

Changing the overall sign of the propagator eliminates the oscillating factor $(-1)^{n-1}$ in the n-pomeron contribution to the reggeon unitarity (all terms in the unitarity condition for $-f_j$ enter with positive sign).

For the vertices we choose

$$(14.1b)$$

Let us stress that the two four-particle vertices would have been identical in a relativistic theory; here they are not, $\lambda \neq \lambda_1$.

In the expression for the scattering amplitude

$$A(s, q^2) = s \int \frac{d\omega}{2\pi i} \xi_j \, \mathrm{e}^{\omega \xi} f_j(q^2), \quad \xi = \ln s,$$

expanding the signature factor ξ_j at small ω values,

$$\xi_j = -\frac{\mathrm{e}^{-i\frac{\pi}{2}j}}{\sin \frac{\pi}{2}j} = i \frac{\mathrm{e}^{-i\frac{\pi}{2}\omega}}{\cos \frac{\pi}{2}\omega} \simeq i + \frac{\pi}{2}\omega,$$

the real part of the amplitude is conveniently represented by the derivative of the imaginary part,

$$A(s, q^2) \simeq \left[i + \frac{\pi}{2} \frac{\partial}{\partial \xi} \right] \operatorname{Im} A(s, q^2). \qquad (14.2a)$$

Therefore it suffices to know the imaginary part. We will calculate the function

$$F(\xi, q^2) \equiv \frac{1}{s} \operatorname{Im} A(s, q^2),$$

whose Fourier transform, $f(\omega, q^2)$, is given by the sum of diagrams with reggeon propagators and vertices (14.1)

$$F(\xi, \mathbf{k}^2) = - \int \frac{d\omega}{2\pi i} \, \mathrm{e}^{\omega \xi} f(\omega, \mathbf{k}^2). \qquad (14.2b)$$

14.1.1 Reggeons and branchings in the impact parameter space

We start from the contribution of the non-enhanced branchings,
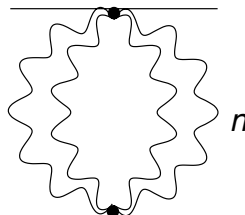
$$f(\omega, \mathbf{k}^2) = -\sum_{n=1}^{\infty} \int \frac{d\omega_1 \ldots d\omega_n \, d^2\mathbf{k}_1 \ldots d^2\mathbf{k}_n}{n! \, [(2\pi)^3 i]^n} G(\omega_1, \mathbf{k}_1) \cdots G(\omega_n, \mathbf{k}_n)$$

$$\cdot (2\pi)^3 \, i\delta(\omega - \sum \omega_i) \delta\left(\mathbf{k} - \sum \mathbf{k}_i\right) N_n^2(\omega_i, \mathbf{k}_i). \qquad (14.3)$$

The fact that this diagram is *not enhanced* means that the vertex blocks N_n are not singular and at small ω and k values, they can be replaced by some numbers, $N_n \approx \mathrm{const}$.

By using the Fourier transformation to the impact parameter space,

$$(2\pi)^2 \delta(\mathbf{k} - \sum \mathbf{k}_i) = \int d^2\boldsymbol{\rho} \, e^{i\mathbf{k}\cdot\boldsymbol{\rho} - i\sum \mathbf{k}_i \cdot \boldsymbol{\rho}},$$

we factorize the transverse momentum integrations to get

$$F(\xi, \mathbf{k}^2) = -\sum_{n=1}^{\infty} \frac{1}{n!} \int d^2\boldsymbol{\rho} \, e^{i\mathbf{k}\cdot\boldsymbol{\rho}} \left(\int \frac{d\omega_1}{2\pi i} \, e^{\omega_1 \xi} \int \frac{d^2\mathbf{k}_1}{(2\pi)^2} G(\omega_1, \mathbf{k}_1) \, e^{-i\mathbf{k}_1 \cdot \boldsymbol{\rho}} \right)^n.$$

The integrals over ω_i run along the imaginary axis,

$$\int \frac{d\omega_1}{2\pi i} \, e^{\omega_1 \xi} G(\omega_1, \mathbf{k}_1) = -\int \frac{d\omega_1}{2\pi i} \frac{e^{\omega_1 \xi}}{\omega_1 + \alpha' \mathbf{k}_1^2} = -e^{-\alpha' \mathbf{k}_1^2 \xi}.$$

Integrating over $\mathbf{k}_1$ we have

$$-\int \frac{d^2\mathbf{k}_1}{(2\pi)^2} \, e^{-\alpha' \mathbf{k}_1^2 \xi - i\mathbf{k}_1 \cdot \boldsymbol{\rho}} = -\int \frac{d^2\mathbf{k}_1}{(2\pi)^2} \, e^{-\alpha' \xi \left(\mathbf{k}_1 + \frac{i\boldsymbol{\rho}}{2\alpha'\xi}\right)^2 - \frac{\boldsymbol{\rho}^2}{4\alpha'\xi}}$$

$$= -\frac{1}{4\pi\alpha'\xi} \exp\left\{-\frac{\boldsymbol{\rho}^2}{4\alpha'\xi}\right\} \equiv \tilde{G}(\xi, \boldsymbol{\rho}). \qquad (14.4)$$

The function $\tilde{G}(\xi, \rho)$ is an important distribution whose physical meaning we will discuss later in this lecture.

Substituting (14.4) into the n-reggeon branching amplitude,

$$F^{(n)}(\xi, \mathbf{k}^2) = -(-1)^n \frac{N_n^2}{n!} \int d^2\boldsymbol{\rho} \, e^{i\mathbf{k}\cdot\boldsymbol{\rho}} \frac{1}{(4\pi\alpha'\xi)^n} \, e^{-\frac{n\boldsymbol{\rho}^2}{4\alpha'\xi}}$$

$$= \frac{N_n^2}{nn!} \frac{(-1)^{n-1}}{(4\pi\alpha'\xi)^{n-1}} \int d^2\boldsymbol{\rho} \, e^{i\mathbf{k}\cdot\boldsymbol{\rho}} \cdot \frac{-n}{4\pi\alpha'\xi} \, e^{\frac{-n\boldsymbol{\rho}^2}{4\alpha'\xi}},$$

we observe that the integrand here is the one we have just calculated above, i.e. the Fourier transform of the Green function $G(\xi, \mathbf{k})$, with the only difference that α' is substituted by α'/n. Hence, we obtain

$$F^{(n)}(\xi, \mathbf{k}^2) = \frac{(-1)^{n-1} N_n^2}{nn!(4\pi\alpha'\xi)^{n-1}} \, e^{-\frac{\alpha'}{n}\mathbf{k}^2\xi}. \qquad (14.5)$$

In the particular case of $n = 1$ we recover the pole expression, $F^{(1)} = e^{-\alpha' \mathbf{k}^2 \xi}$. What is the magnitude of the nth branching contribution like? Is it large or small?
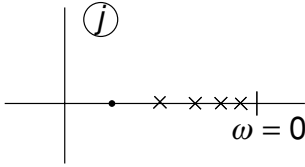
The (modulus of the) exponent in (14.5) is at its maximum for $n = 1$, i.e. the contributions of the branchings, $n \geq 2$, are *larger* than that of the pole, in the sense of the position of the singularity in the j-plane. On the other hand, the first term is larger owing to the suppression of the higher terms by the pre-exponential factor $F^{(n)} \propto 1/\xi^{n-1}$. Thus one cannot state a priori that $n \to \infty$, $j_n \to 1$ are the most important contributions.

14.1.2 Qualitative estimate of the series

Let us try to estimate the sum

$$F = \sum_n F^{(n)}(\xi, \mathbf{k}^2). \tag{14.6}$$

Our estimate is going to be rough since the we don't know the dependence of the vertex functions N_n on n, and other – enhanced – diagrams are important too. Nevertheless, just for curiosity's sake, let us look at which n are relevant in the series (14.6).

If $\mathbf{k}^2 = 0$, everything is very simple: all singularities are at the same point $j = 1$ and the pole dominates:

$$F(\xi, \mathbf{k}^2) = g^2 - \frac{N_2^2}{4\pi\alpha'\xi} + \mathcal{O}\left(\xi^{-2}\right).$$

This is true not only for $\mathbf{k}^2 = 0$, but in an interval of momenta where the condition $\alpha' \mathbf{k}^2 \xi \ll 1$ is satisfied.

In the opposite case, when $\alpha' \mathbf{k}^2 \xi \gg 1$, the far terms of the series become important. How can we estimate the sum? It is clear that one has to find $n = n_{\max}$ which marks the maximal contribution, $\max_n\{F_n\} = F_{n_{\max}}$.
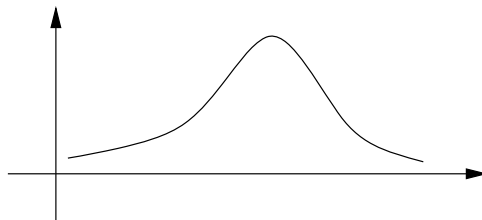
Since the number of relevant terms is large, we can write

$$F \simeq \sum_n e^{\varphi(n)} \simeq \int dn\, e^{\varphi(n)} ,$$

and attempt to apply the steepest-descent method to the exponent

$$\varphi(n) = -\frac{\alpha' \mathbf{k}^2 \xi}{n} - (n-1)\ln(4\pi\alpha'\xi) - n\ln n + i\pi n, \qquad (14.7)$$

where $-n\ln n$ originated from the combinatorial $1/n!$ factor. There is one delicate point here; the series has alternating signs, therefore the term $i\pi n$ in (14.7). This is not a very sensible way to estimate oscillating series but is good enough to illustrate the key feature of the answer.

The saddle-point equation,

$$\frac{d\varphi(n)}{dn} = \frac{\alpha' \mathbf{k}^2 \xi}{n^2} - \ln(4\pi\alpha'\xi) - \ln n - 1 + i\pi = 0,$$

determines the scale of n at which the terms of the series are large:

$$\frac{\alpha' \mathbf{k}^2 \xi}{n_{\max}^2} = \ln(\alpha'\xi n_{\max}) + \mathcal{O}(1) , \quad n_{\max}^2 \approx \frac{\alpha' \mathbf{k}^2 \xi}{\ln(\alpha'\xi n_{\max})} \sim \frac{2\alpha' \mathbf{k}^2 \xi}{\ln(\xi^3 \mathbf{k}^2)},$$

where we omitted the constant in the argument of the logarithm. Now we approximate $\varphi(n_{\max})$,

$$\varphi(n_{\max}) \sim \sqrt{2\alpha' \mathbf{k}^2 \xi \ln(\xi^3 \mathbf{k}^2)},$$

and obtain the scale of the answer in the region $\alpha' \mathbf{k}^2 \xi \gg 1$:

$$F(\xi, \mathbf{k}^2) \sim F^{(n_{\max})} \sim e^{-c\sqrt{\alpha' \mathbf{k}^2 \xi}}. \qquad (14.8)$$

Here we have dropped the ln factor in the exponent, since our estimation is rough anyway. The decrease of (14.8) with ξ is fast, but *slower* than any exponent, $\exp(-\gamma\xi)$, $\gamma > 0$.

What is the correct way of calculating the sign-alternating series? One has to write down the representation of the Sommerfeld–Watson type,

$$\sum_n (-1)^{n-1} f_n = \frac{1}{2i} \int \frac{dn}{\sin \pi n} f_n ,$$

and include $\ln \sin \pi n$ into the exponent $\varphi(n)$. Its presence produces a pair of complex conjugate points as the saddle-point solution. As a result, in addition to the exponent of $\sqrt{\alpha'\xi k^2}$, the answer also acquires a factor $\cos(\alpha'\xi k^2)$ which leads to *oscillations* in the scattering amplitude.

Let us see, what we obtain by fixing ξ and increasing k:
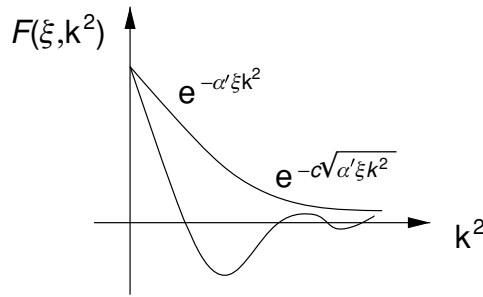
We have here a curious result, just like in classical diffraction: the pole term leads to a diffraction cone; taking into account the branchings, the slope of the amplitude falloff decreases, and oscillations appear.

We can conclude that in the region of small momentum transfers non-enhanced branchings do not alter the pole picture. With the growth of $\mathbf{k}^2$, however, the angular distribution changes drastically; due to the alternating signs of the multi-reggeon branching contributions, maxima and minima appear naturally in the differential scattering cross section.

This would have been the answer, and a rather simple one, if not for enhanced reggeon diagrams.

14.2 Enhanced diagrams for reggeon propagator

To write down everything is impossible, so we restrict ourselves to the simplest interaction . The exact reggeon Green function is given by the sum of diagrams with various reggeon loops the bare reggeon can mix with, and their repetitions,
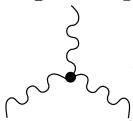
14.2.1 Reggeon loop in the reggeon propagator

Consider the first correction to the propagator:

$$G^{(1)} = \frac{1}{\omega + \alpha' \mathbf{k}^2} \Sigma(\omega, \mathbf{k}^2) \frac{1}{\omega + \alpha' \mathbf{k}^2}, \tag{14.9}$$

$$\Sigma(\omega, \mathbf{k}^2) = r^2 \int \frac{d\omega' \, d^2\mathbf{k}'}{(2\pi)^3 \, i} \frac{1}{\omega' + \alpha' \mathbf{k}'^2} \frac{1}{\omega - \omega' + \alpha'(\mathbf{k} - \mathbf{k}')^2}. \tag{14.10}$$

To calculate the 'self-energy' insertion (14.10) it is natural to take the ω' integral first. The integration contour lies between the two poles; closing the contour around one of them we obtain

$$\Sigma(\omega, \mathbf{k}^2) = r^2 \int \frac{d^2\mathbf{k}'}{(2\pi)^2} \frac{1}{\omega + \alpha' \mathbf{k}'^2 + \alpha'(\mathbf{k} - \mathbf{k}')^2}. \tag{14.11}$$

This is a typical expression for the two-reggeon branching. The first thing we observe is that this integral diverges at $\mathbf{k}^2 \to \infty$. There is nothing strange nor terrible in this, since we treated all the vertices as constants and expanded $\varepsilon(\mathbf{k}^2)$, being interested in region of small transverse momenta. The integration has to be carried out up to a certain value $\mathbf{k}^2_{\max}$.

In any case, not this is the source of our problems. More important is the strong singularity in ω: taking $\omega = 0$, the integral tends to infinity in the limit of *small* momentum transfer, $\mathbf{k}^2 \to 0$. This is a logarithmic divergence corresponding to a branch-cut singularity.

Let us calculate the integral (14.11). Introducing a symmetric integration variable $\mathbf{q}$ such that $\mathbf{k}' = \mathbf{q} + \frac{1}{2}\mathbf{k}$ ($\mathbf{k} - \mathbf{k}' = \mathbf{q} - \frac{1}{2}\mathbf{k}$) we derive

$$\Sigma(\omega, \mathbf{k}^2) = r^2 \int \frac{d^2\mathbf{q}}{(2\pi)^2} \frac{1}{\omega + \frac{1}{2}\alpha' \mathbf{k}^2 + 2\alpha' \mathbf{q}^2} = \frac{r^2}{8\pi\alpha'} \ln \frac{\Lambda}{\omega + \frac{1}{2}\alpha' \mathbf{k}^2}, \tag{14.12}$$

where parameter Λ limits from above the q-integration, $\mathbf{q}^2 \le \Lambda/2\alpha'$. The position of the singularity, $\omega = -\frac{1}{2}\alpha' \mathbf{k}^2 \equiv \omega_2$ is just that of the two-reggeon branching, cf. (11.36).

Let us imagine that we sum up the series of 'self-energy' corrections to the propagator:

$$\begin{aligned} G(\omega, \mathbf{k}^2) &= G_0 + G_0 \Sigma G_0 + G_0 \Sigma G_0 \Sigma G_0 + \cdots = G_0 + G_0 \Sigma \cdot G \\ &= \frac{1}{G_0^{-1} - \Sigma(\omega, \mathbf{k}^2)} = -\frac{1}{\omega + \alpha' \mathbf{k}^2 + \Sigma(\omega, \mathbf{k}^2)} . \end{aligned} \tag{14.13}$$

We obtained an expression not having any pole at $\omega \simeq 0$ at small $\mathbf{k}^2$ values; the correction (14.12) is huge (*infinite* at $\omega \propto \mathbf{k}^2 \to 0$). What happened could have been foreseen: when the pole is on the cut, in the same point as the branchings, one cannot expect to get anything nice.

$$\left(k^2\right) \quad \textit{Reggeon field theory}$$

$$\overset{\times}{m^2} \qquad 4m^2 \qquad 9m^2$$
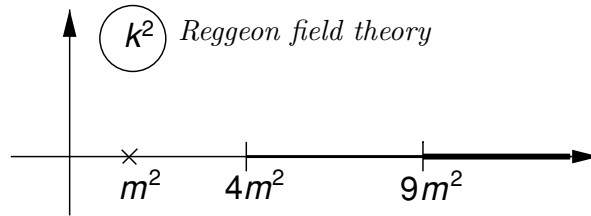
Fig. 14.1   The particle pole and multi-particle branch cuts in QFT with $m \neq 0$.

14.2.2 Analogy with $m = 0$ infrared singularity in QFT

What phenomenon in the field theory could correspond to this catastrophe? Recall the usual ϕ^3 field theory. What sort of singularities did we have there? The bare Green function contained the mass parameter m_0; the corrections lead to the appearance of the renormalized mass m entering observable phenomena. In the momentum transfer plane the particle pole is separated from threshold branchings as shown in Fig. 14.1.

In order to feel the analogy, let us imagine that the intercept of our pomeron is not exactly unity: $\alpha_{\mathbf{P}}(0) \neq 1$.

$$j \simeq \alpha(0) + \alpha' \mathbf{k}^2 \, , \qquad \omega = \alpha(0) - 1 - \alpha' \mathbf{k}^2 = \Delta - \alpha' \mathbf{k}^2.$$

In this case the multi-pomeron branchings would be in the points

$$\omega_n = n\Delta - \frac{\alpha' \mathbf{k}^2}{n}.$$

If $\Delta < 0$, higher branchings move away from the pole, and the structure of singularities displayed in Fig. 14.2 is analogous to that in particle theory (Fig. 14.1). In terms of particles $\Delta \to 0$ means that the *mass* of the particle is approaching zero. What would happen in field theory then? The same trouble as in our pomeron problem.

Take $m_0 = 0$ in the particle propagator,

$$G_0 = \overline{} = \frac{1}{-k^2} \, ;$$

the first self-energy correction $\overline{}\bigcirc\overline{}$ gives $G = -(\mathbf{k}^2 + \Sigma(\mathbf{k}^2))^{-1}$. Generally speaking, the pole at $k^2 = 0$ would disappear – the particle
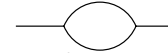
$$\left(\omega\right)$$
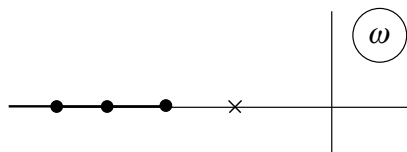
Fig. 14.2   Regge pole $\alpha(0) - 1 = \Delta < 0$ and corresponding branchings.

acquires a mass, if only one does not take special measures to prevent it from doing so. We have met such a situation in electrodynamics:

$$D^0_{\mu\nu}(k) = \frac{g_{\mu\nu}}{k^2} \quad \implies \quad D_{\mu\nu}(k) = \frac{g_{\mu\nu}}{k^2 + \Pi(k^2)} \ .$$

Making use of the conservation of electromagnetic current we have shown that the polarization operator vanishes in the origin, $\Pi(k^2) \propto k^2$ at $k^2 \to 0$. In this sense we can say that the photon did not acquire a mass owing to the symmetry – to gauge invariance in this case.

We see that our situation with $\alpha_{\mathbf{P}}(0) = 1$ is just the same; taking the bare Green function with zero mass, the corrections diverge. This is actually the main problem of the theory of interacting pomerons. We do not know, have not formulated any reason *why* the total cross sections are asymptotically constant. Having not understood this, having not imposed the additional condition, we will always face the problem that the pole does not 'hold' at $\alpha(0) = 1$.

Can it go to the right? No, since we took into consideration the branchings and respected the Froissart theorem which forbade the power growth of the total cross section. However, there is no way to prevent it from *decreasing* with energy.

Indeed, it is easy to see that the pole bounces to the left, since, owing to the anti-hermiticity of the theory, the correction to the position of the singularity comes with a negative sign,

$$\delta\omega_0 = -\frac{r^2}{8\pi\alpha'} \ln\frac{\Lambda}{\omega_0} < 0.$$

Consequently, without understanding *why* the cross section is constant, we cannot ensure the self-consistence of the theory.

14.3 $\sigma_{\mathbf{tot}} \simeq$ const as an infrared singular point

We have come to two conclusions, namely that

(1) the pomeron pole does not stay at $\alpha_{\mathbf{P}} = 1$; and

(2) taking into account the simplest interactions, it shifts *to the left*.

Nevertheless the question arises what Green function and interaction vertices do we have to use in order to have the *renormalized* pole at 1. Evidently, the initial position of the pole has to be chosen to the right

from unity:

$$G_0 = \frac{-1}{\omega - \Delta + \alpha' \mathbf{k}^2}, \quad \Delta = \alpha(0) - 1 > 0.$$

This, however, does not solve the problem. Indeed, inside the two-reggeon loop Σ we have to use the *renormalized* poles, in order to avoid the self-energy corrections to the loop propagators,

$$\Sigma = r^2 \int \frac{d^2\omega \, d^2 \mathbf{k}'}{(2\pi)^3 i} G(\omega', \mathbf{k}') G(\omega - \omega', \mathbf{k} - \mathbf{k}'). \tag{14.14}$$

The exact Green functions, however, are supposed to have poles in the origin, $\omega \propto \mathbf{k}^2 \to 0$, and the loop integral acquires singularity at the point where the two poles pinch,

$$-\alpha' \mathbf{k}'^2 = \omega + \alpha'(\mathbf{k} - \mathbf{k}')^2;$$
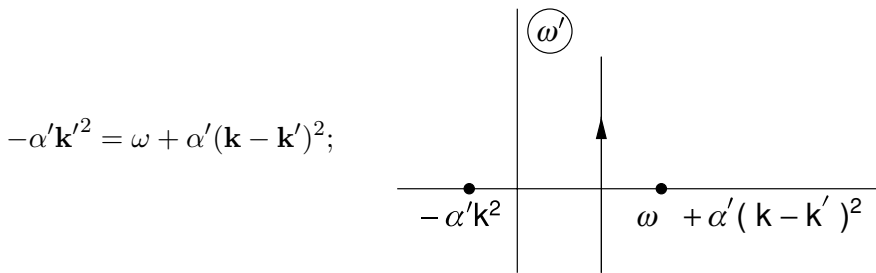
The condition for the pinch in $\mathbf{k}'$ gives $\omega + \frac{1}{2}\alpha'\mathbf{k}^2 = 0$, and we get

$$G(\omega, \mathbf{k}^2) = -\left(\omega - \Delta + \alpha' \mathbf{k}^2 + \frac{r^2}{8\pi\alpha'} \ln \frac{\Lambda}{\omega + \frac{1}{2}\alpha'\mathbf{k}^2} \right)^{-1}. \tag{14.15}$$

We see that $\Delta > 0$ did not help: the infrared singularity is *too strong* to be taken care of by mere introduction of a constant shift in the position of the bare pole. One has to look deeper, to take into account more complicated diagrams, to address the question of the possible behaviour of the renormalized vertices, etc.

We face the following problem: *what the Green function has to be in order to ensure that the theory contains a massless excitation?*

This is a general question which appears also in the condensed matter physics context. In our case it is about $\mathbf{P}$ in 1.

14.3.1 Corrections to the vertex part

Before we start summing the diagrams, let us see what is the scale of the correction to the *vertex* (as we will discover shortly, it is actually the

vertex that plays a determining rôle).

$$\Gamma \equiv \quad = \quad + \quad + \cdots$$
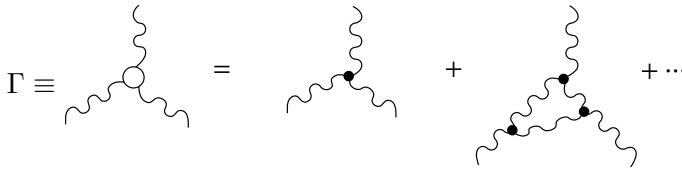
In terms of renormalized reggeon Green functions, the first correction takes the form

$$\Gamma_2 \quad = \quad \simeq \quad r^3 \int \frac{d\omega'\, d^2\mathbf{k}'}{(2\pi)^3\, i} \frac{1}{\omega' + \alpha'\mathbf{k}'^2}$$

$$\cdot \quad \frac{1}{\omega - \omega' + \alpha'(\mathbf{k} - \mathbf{k}')^2} \cdot \frac{1}{\omega' - \omega_1 + \alpha'(\mathbf{k}' - \mathbf{k}_1)^2}. \quad (14.16\text{a})$$

Now at large $\mathbf{k}'^2$ values everything is all right. We will estimate this expression by simply counting the powers. Let all the external variables be of the same order of magnitude, $\omega_1 \sim \omega_2 \sim \alpha'\mathbf{k}_{1,2}^2 \sim \alpha'\mathbf{k}^2 \sim \omega$. Then

$$\Gamma_2 \sim \frac{r^3}{\omega}, \qquad \frac{\Gamma_2}{r} \sim \frac{\delta\Gamma}{\Gamma} \sim \frac{r^2}{\omega}. \quad (14.16\text{b})$$

For $\omega > r^2$ the correction is small, and we can use perturbation theory all right. However, at small values of ω, $\omega < r^2$, we face a rather catastrophic situation: the correction becomes large, and diverges in the $\omega \to 0$ limit.

What happens here is almost identical to the problem of the second-order phase transitions ('almost' because our specific problem is marked by the anti-Hermiticity of the effective Hamiltonian). Normally, correlation functions in a thermodynamical system fall exponentially with the distance,

$$\int d^3\mathbf{k} \frac{e^{i\mathbf{k}\cdot\mathbf{r}}}{\mathbf{k}^2 + \Delta^2} \sim \frac{e^{-\Delta r}}{r}. \quad (14.17)$$

If at a certain temperature T the value of Δ turns to zero, the correlation radius goes to infinity, and the system undergoes the phase transition. At temperatures close to the critical, $T \approx T_c$, the excitations interact strongly and the perturbation theory becomes divergent.

Historically, the understanding of the problems of interacting pomerons and of the second order phase transitions in condensed matter physics was being gained practically simultaneously. The two problems turn out to be

very similar; the only difference is that, let us stress it again, the pomeron dynamics corresponds effectively to an anti-Hermitian Hamiltonian.

14.3.2 Equations for the renormalized vertex and the reggeon propagator

What can be said about the exact vertex? It can be shown that all the diagrams for the corrections to the vertex part can be combined into *skeleton diagrams* built of *exact* Green functions and vertices. (Skeleton diagrams are those which contain no block that would represent a correction to an internal vertex.)

$$\tag{14.18}$$

This is one equation for two quantities, the propagator and the vertex. A second equation seems to be easy to write – the Dyson equation,

$$G(\omega, \mathbf{k}) \; = \; G_0(\omega, \mathbf{k}) \; + \quad \text{} \; . \tag{14.19}$$

The impression that this equation may be more informative than that for the vertex function (14.18), containing an infinite number of terms, is deceiving. In fact, (14.19) is *not an equation*: the loop integral diverges, and the expression contains $G(\mathbf{q})$ and $\Gamma(\mathbf{q}, \mathbf{q}, \mathbf{k})$ in the region of large momenta $\mathbf{q}$ about which we do not know anything.

One usually performs the *renormalization*. This, however, does not solve the problem but rather hides it. At the same time, there is a simple way to derive the second equation we need. Indeed, the divergence is a consequence of the fact that G is a 'dimensional' quantity: $[G] \sim 1/\omega$. It is sufficient therefore to take a derivative and write down an equation for the 'dimensionless' quantity $\partial G^{-1}(\omega, \mathbf{k})/\partial \omega$.

Imagine one of the diagrams participating in Σ, . The external 'energy' ω flows through some of the internal lines. Differentiation over ω leads to *doubling* one of these internal lines,

$$\frac{\partial}{\partial \omega} \frac{1}{(\omega - \sum_k \omega_k' + \cdots)} \; = \; -\frac{1}{(\omega - \sum_k \omega_k' + \cdots)} \cdot \frac{1}{(\omega - \sum_k \omega_k' + \cdots)} ,$$

and resembles the vertex with zero 'energy–momentum' transfer,

$$\frac{\partial}{\partial\omega}\ \left(\ \underline{\quad\quad}\ \right)\ =\ -\ \underline{\quad\otimes\quad}\ \cdot$$

Indeed, it can be checked that the equation for the derivative of the inverse reggeon Green function looks diagrammatically exactly the same as the equation for the exact vertex:

$$\frac{\partial G^{-1}}{\partial\omega}\ \equiv\ \otimes\ =\ -1\ +\ \ +\ \ +\cdots \qquad (14.20)$$

Unfortunately, equations (14.18) and (14.20) are represented in the form of infinite series. Therefore, there is always a danger that, owing to the possible divergence of the series, conclusions that one would derive from these equations may turn out to be wrong.

14.4 Weak and strong coupling regimes

Leaving aside the problem of the convergence of the series, we can guess the structure of the solution. But first, having expressed the equations for the vertex (14.18) and the propagator (14.20) in terms of *exact*, renormalized quantities, we have to re-examine the size of corrections. In other words, we have to estimate the magnitude of the effective expansion parameter.

Each subsequent term on the r.h.s. of the equation contains, compared to the previous one, three reggeon Green functions, two vertices and an additional integration over the reggeon loop:

$$\frac{\delta\Gamma}{\Gamma}\ \sim\ \frac{\delta\Sigma}{G^{-1}}\ \sim\ \int d^2\mathbf{k}'\,d\omega'\,G^3\Gamma^2\ \sim\ e^2. \qquad (14.21a)$$

We may represent this parameter as

$$e^2\ \sim\ \frac{\langle\mathbf{k}^2\rangle}{\omega}\cdot\left(\omega G\right)^3\cdot\frac{\Gamma^2}{\omega}, \qquad (14.21b)$$

with $\langle\mathbf{k}^2\rangle$ the characteristic transverse momentum in the integral. If renormalization effects were moderate and did not drastically change the behaviour at small ω, so that $\Gamma\sim r$, $\omega G\sim 1$, $\langle\mathbf{k}^2\rangle\sim\omega$, this would lead us back to the original estimate (14.16b), $e^2\sim r^2/\omega$.

The quantity e^2 depends on the external variables ω, $\mathbf{k}^2$ and can be looked upon as the 'invariant charge' – the true measure of the 'interaction strength' in the theory of interacting pomerons. Our theory may have a

self-consistent solution in two regimes, characterized by the magnitude of
the 'invariant charge' in the $\omega \to 0$ limit:

- Weak coupling, $e^2 \ll 1$. This regime is possible if the interaction
  modifies the interaction vertex so that Γ *vanishes* when $\mathbf{k}^2 \to 0$,
  $\omega \to 0$. Given a small effective interaction strength, one can use per-
  turbative expansion to control the corrections.

- Strong coupling, $e^2 \sim 1$. In this case all terms in the equations are of
  the same order, and perturbation theory is not applicable.

14.4.1 Scaling solution. Strong coupling

We have seen that having taken the bare quantities and having started
the iterations of the equation, we have obtained the growing corrections.
How can we, nevertheless, make the l.h.s. and the r.h.s. of the equation
equal?

Since correction terms appear to be singular in the origin, let us sup-
pose that the *bare terms* could be neglected in the equations. If so, we
would arrive at a homogeneous non-linear integral equation for the sin-
gular quantities (while the constant bare terms may be cancelled by non-
singular pieces of the skeleton diagrams on the r.h.s.).

When we search for a self-consistent solution, not only the matching of
numerical values of the l.h.s. and r.h.s. of the equation is required, but also
that of the *singularities*. If the singularity is weak, then the perturbation
theory can be used. If, on the contrary, the singularity is strong, then the
Born terms drop out and we get a homogeneous equation.

Bearing in mind the second case, let us look for a solution in the fol-
lowing form:

$$G(\omega, \mathbf{k}^2) \;\;=\;\; \omega^\mu g\left(\frac{\mathbf{k}^2}{\omega^\nu}\right), \tag{14.22a}$$

$$\Gamma(\omega, \mathbf{k}^2; \omega_1, \mathbf{k}_1^2; \omega_2, \mathbf{k}_2^2) \;\;=\;\; \omega^\rho \gamma\left(\frac{\mathbf{k}_1^2}{\omega_1^\nu}, \frac{\mathbf{k}_2^2}{\omega_2^\nu}, \frac{\mathbf{k}^2}{\omega^\nu}, \frac{\omega_1}{\omega}\right). \tag{14.22b}$$

This is a statement of the 'scaling' type: we extracted the overall powers
of ω and introduced the functions g and γ depending only on the *ratios*
of all other variables. We have to substitute this scaling solution in the
equation (omitting the finite bare terms) and see if it reproduces itself
under iterations.

It is clear that the 'homogeneous matching' can be achieved only if
$e^2 \sim 1$. Substituting (14.22) into, for example, the equation for Γ, the

first diagram in (14.18) gives

$$\Gamma \; \simeq \; \int \frac{d\omega'\, d^2\mathbf{k}'}{\omega'\ \omega'^\nu} \cdot (\omega')^{\nu+1} \big(\omega'^\mu g\big)^3 \big(\omega'^\rho \gamma\big)^3. \qquad (14.23)$$

Due to the scale invariance of the functions g and γ in (14.22) under the transformation

$$\omega \to \lambda\omega, \qquad \mathbf{k}^2 \to \lambda^\nu \mathbf{k}^2,$$

the integral (14.23) will behave as $\lambda^{3(\rho+\mu)+\nu+1}$. This means that it can always be written in the form

$$\Gamma \; \simeq \; \omega^{3(\mu+\rho)+\nu+1} F(\text{ratios})$$

(provided the integral is convergent). Now, equating the exponents, our only requirement is that the relation $\rho = 3(\mu+\rho) + \nu + 1$ should be satisfied:

$$3\mu + 2\rho + \nu + 1 \; = \; 0.$$

Let us note that this condition actually means $e^2 = \mathcal{O}(1)$. Indeed,

$$e^2 \sim \int d^2\mathbf{k}\, d\omega\, G^3 \Gamma^2 \; \sim \; \omega^{\nu+1}\omega^{3\mu}\omega^{2\rho}\, \Phi(\text{ratios}) \; = \; \text{const.}$$

This shows that in the scaling solution the 'effective charge' e^2 does not depend on the small quantity ω. Hence, $e^2 \sim 1$, corresponding to the *strong coupling* regime.

It can be easily verified that in *all* diagrams in the equations for the Green function and the vertex, the scaling solution (14.22) reproduces itself.

Our equations in the strong coupling regime do not contain parameters at all. The phase space volume $d^2\mathbf{k}\, d\omega \sim (d^3k)$ is the only quantity which reflects the specific features of the theory. K. Wilson suggested an interesting method for the investigation of such equations, namely, the continuation in the *number of dimensions*. By treating the deviation (ϵ) from the actual number of dimensions (three in our case) as a small parameter, one can approximate the solution by series in ϵ.

14.4.2 The cross section seems to change inevitably

Let us demonstrate that the scaling ('strong coupling') solution is incompatible with the $\sigma_{\text{tot}} \to \text{const}$ asymptotic behaviour. Evaluating the imaginary part of the reggeon Green function to get the total cross section

we obtain

$$\sigma_{\text{tot}}(\xi) \propto \text{Im}\, A(\xi, \mathbf{k}^2 = 0) \sim \int d\omega\, e^{\omega \xi} \cdot \omega^\mu \propto \xi^{-(\mu+1)}. \qquad (14.24)$$

Consider first the case $\mu + 1 > 0$ corresponding to the total cross section *decreasing* with energy. In this case,

$$\frac{\partial G^{-1}}{\partial \omega} \to \infty \quad (\omega \to 0),$$

so that the bare term (-1) in (14.20) for the derivative of the inverse pomeron Green function can be neglected. But then my equations would not know that the Hamiltonian of my theory was actually anti-Hermitian: with the Born terms dropped, the equations become insensitive to the sign of G. A solution with $G > 0$ would not satisfy us, since in this case the contributions of the branchings would be of the same sign, and the unitarity condition would be not of the reggeonic type. The series must be alternating, corresponding to $G < 0$. As a more detailed analysis shows, there is no satisfactory solution for $\mu + 1 > 0$.

Now we take $\mu + 1 < 0$:

$$\frac{\partial G^{-1}}{\partial \omega} \to 0 \quad (\omega \to 0).$$

Now the unity can not be thrown away in the equation. In this case a solution exists corresponding to $G < 0$. This means that the total cross sections might *grow logarithmically* with energy.

Neither of the two cases is what we have been looking for. The scaling solution does not allow us to have a constant cross section, $\mu + 1 = 0$. In fact, all negative integer μ values are forbidden by the strong coupling equations.

How can this be seen? If $\mu = -1$, in the $\omega \to 0$ limit we have

$$\frac{\partial G^{-1}}{\partial \omega} \sim \omega^0 = \text{const.} \qquad (14.25)$$

Will this constant be reproduced by the equation (14.20)?

Let us consider the simplest diagram,

$$\Delta \frac{\partial G^{-1}}{\partial \omega} = \quad \sim \int d\omega' \, d^2\mathbf{k}' \frac{\partial G^{-1}}{\partial \omega} G^3 \Gamma^2,$$

and rewrite the integrand as follows,

$$\int \frac{d\omega'}{\omega'} \frac{\partial G^{-1}}{\partial \omega} \left[d^2\mathbf{k}' \cdot \omega' \cdot G^3 \Gamma^2 \right] \sim \int \frac{d\omega'}{\omega'} \frac{\partial G^{-1}}{\partial \omega} \cdot e^2. \qquad (14.26)$$

Since $e^2 = \mathcal{O}(1)$, substituting the constant for the derivative of G leads to a logarithmic divergence,

$$\Delta \frac{\partial G^{-1}}{\partial \omega} \simeq \text{const} \int \frac{d\omega'}{\omega'} \propto \ln \omega,$$

incompatible with the assumption (14.25). This is a general feature of dimensionless integrals.

14.4.3 How to enforce $\sigma_{\text{tot}} \simeq$ const? Weak coupling

The question arises, whether, in fact, the cross section can be still asymptotically constant? What would be necessary to achieve such a behaviour? We have to force the corrections to be small, despite the divergence of the perturbation corrections.

We have supposed that the three-reggeon vertex is finite, $\Gamma = \mathcal{O}(1)$, and estimated the contribution of the reggeon loop in (14.16) as $\delta\Gamma \propto \omega^{-1}$ – this is, obviously, not suitable. However, if we took for the renormalized vertex Γ an expression that *vanishes* with $\omega, \mathbf{k} \to 0$,

$$= a\omega + b\left(\mathbf{k}_1^2 + \mathbf{k}_2^2\right) + c\mathbf{k}^2, \qquad (14.27)$$

we might achieve the matching.

If the increasing solution is analogous to that in phase transitions, the present – *weak coupling* – situation corresponds to quantum electrodynamics: the photon does not acquire a mass because its emission vertex contains momenta in the numerator:

$$\Pi_{\mu\nu} = (k_\mu k_\nu - g_{\mu\nu} k^2)\Pi(k^2) \implies m_\gamma = 0.$$

Up to now we have considered only the three-pomeron vertex. For the self-consistence of the weak-coupling picture it is necessary and sufficient

that the four-reggeon interaction vertices in (14.1b) also vanish in the origin, $\lambda, \lambda_1 \to 0$ with $\omega_i, \mathbf{k}_i \to 0$.

It can be shown that all possibilities for the solutions of the interacting pomeron problem are exhausted by the described above cases of 'strong' and 'weak' coupling.

A few words about the structure of the j-plane in the two regimes.

Weak coupling. The pomeron Green function,

$$G(\omega, \mathbf{k}^2) = -\frac{1}{\omega + \alpha' \mathbf{k}^2 - \Sigma(\omega, \mathbf{k}^2)}, \quad \Sigma(\omega, \mathbf{k}^2) \sim \; \; \Gamma \; \bigcirc \; \Gamma, \quad (14.28a)$$

acquires a small but *complex* self-energy term, $\Sigma \propto \mathbf{k}^4$. Owing to the complexity of the correction, the initial pole transforms into two conjugate

poles. (If the theory were Hermitian, these poles would have had to move onto an unphysical sheet.) Apart from these poles, we have a family of branch cuts accumulating to $\omega = 0$.
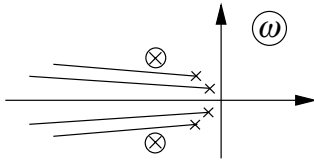
Strong coupling. Here the Green function contains branch point singularities embedded from the start, due to its complicated structure,

$$G(\omega, \mathbf{k}^2) = \omega^\mu g\left(\frac{\mathbf{k}^2}{\omega^\nu}\right). \qquad (14.28b)$$

For $t > 0$ all singularities are on the right of, and condensing to, $\omega = 0$; at $t = 0$ they form a continuous cut starting at $\omega = 0$. In the physical region, $t < 0$, this cut is accompanied by a strong accumulation of branch cuts, whose presence strongly affects the angular dependence of the scattering amplitude. We made the hypothesis that

the vacuum Pomeranchuk pole (pomeron $\mathbf{P}$) exists and studied the total cross section, and amplitudes of elastic and quasi-elastic processes of production of a small number of particles with large rapidity gaps between them. From this study a picture has emerged in which one has to include, apart from the pole $\mathbf{P}$, also branchings, both non-enhanced,
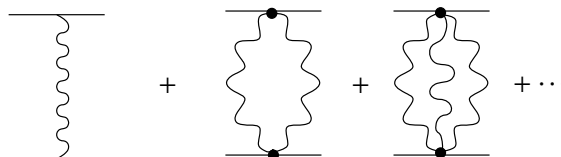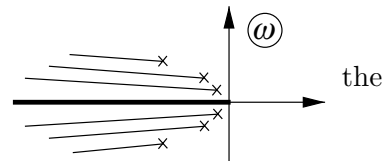
and enhanced
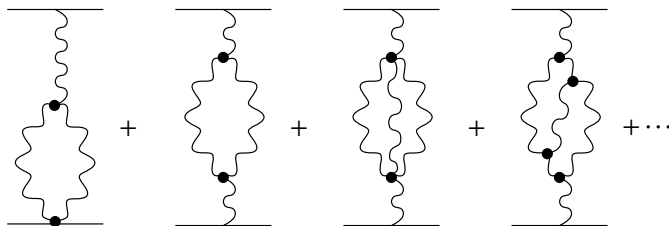
We have found two scenarios that may lead to a self-consistent solution of the problem of interacting pomerons.

(1) If we insist on $\sigma_{\text{tot}} \to \text{const}$ in the $s \to \infty$ asymptotics, then we need to consider the weak coupling regime (14.28a) characterized by vanishing three- and four-pomeron vertices, see (14.27).

(2) If we release the asymptotic *constancy* condition and allow the total cross section to increase logarithmically, $\sigma_{\text{tot}} \sim \ln^a s$ with $a \leq 2$, then we may turn to the strong coupling regime (14.28b).

One may think that in both scenarios it is the simplest graph that mainly determines the cross sections, while the multi-pomeron diagrams provide controllable corrections.

14.5 Weak and strong coupling: view from the s channel

Now we are going to formulate our results in terms of rapidities and impact parameters. Then we will turn to the main question: how the picture of interacting pomerons manifests itself in the s-channel. For example, what s-channel processes correspond to G in the strong coupling regime?

Let us make, first of all, a technical remark. Recall representation (14.2) for the scattering amplitude,

$$A(s, \mathbf{k}^2) = s \left(i + \frac{\pi}{2} \frac{\partial}{\partial \xi} \right) \int \frac{d\omega}{2\pi i} \, e^{\omega \xi} f(\omega, \mathbf{k}^2), \qquad (14.29)$$

where $f(\omega, \mathbf{k}^2)$ is the sum of reggeons diagrams. Recalling that ω lies on the imaginary axis, this integral can be considered as the transition from the frequency to the time representation. In this representation, the image of the pomeron propagator,

$$G(\xi, \mathbf{k}^2) = -e^{-\alpha' \mathbf{k}^2 \xi} \theta(\xi),$$

resembles the Green function $G(t) = \exp(-i(k^2/2m)t)\theta(t)$ describing a free non-relativistic particle, with $\xi = \ln s$ the analogue of (imaginary) time.

Since there is a full analogy with time, an arbitrary diagram can be written without any calculations, using the rules of non-relativistic field theory. For example, for a semi-enhanced diagram with the transition of one reggeon into two, we introduce integration over the transition 'time' ξ_2 to write
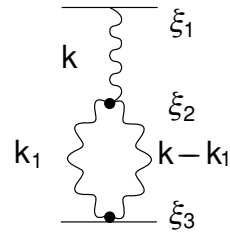
$$g \int_{\xi_3}^{\xi_1} d\xi_2 \, G(\xi_1 - \xi_2, \mathbf{k}) \int \frac{d^2\mathbf{k}_1}{(2\pi)^2} r G(\xi_2 - \xi_3, \mathbf{k}_1) G(\xi_2 - \xi_3, \mathbf{k} - \mathbf{k}_1) N.$$

14.5.1 Diffusion in the impact parameter space

One can go even further, moving to the transverse coordinates, see (14.4):

$$\tilde{G}(\xi, \boldsymbol{\rho}) = \int \frac{d^2\mathbf{k}}{(2\pi)^2} \, \mathrm{e}^{-i\mathbf{k}\cdot\boldsymbol{\rho}} G(\xi, \mathbf{k}) = -\frac{\mathrm{e}^{-\boldsymbol{\rho}^2/4\alpha'\xi}}{4\pi\alpha'\xi} \, .$$

Once again, this is the Green function of a non-relativistic particle propagating in imaginary time $t = i\xi$, or, better to say, the Green function of an equation describing *two-dimensional diffusion*.

Let us consider in these terms the simplest non-enhanced branching:

$$= \; g^2 \tilde{G}(\xi_1 - \xi_2, \boldsymbol{\rho}_1 - \boldsymbol{\rho}_2), \tag{14.30a}$$

$$= \; N^2 \tilde{G}^2(\xi_1 - \xi_2, \boldsymbol{\rho}_1 - \boldsymbol{\rho}_2). \tag{14.30b}$$

In this language, the expression for the two-reggeon branching (14.30a) is no more difficult to put down than that for one reggeon, (14.30a). This also makes it immediately clear, why the branching contributes less than the pole.

Consider the contribution to σ_{tot}, which corresponds to setting $\mathbf{k} = \mathbf{0}$. Then in the impact parameter space representation we need to evaluate

the integral

$$\int \tilde{G}^2(\xi, \boldsymbol{\rho})\, d^2\boldsymbol{\rho} \;=\; \int d^2\boldsymbol{\rho}\, \frac{\mathrm{e}^{-2\cdot\boldsymbol{\rho}^2/4\alpha'\xi}}{(4\pi\alpha'\xi)^2}.$$

In the pomeron propagation, characteristic impact parameters grow with 'time', $\boldsymbol{\rho}^2 \sim \alpha'\xi$, but the normalization in (14.30) is chosen such that $\int \tilde{G}(\xi, \boldsymbol{\rho})\, d^2\boldsymbol{\rho} = -1$ (by the very nature of the Green function). So,

$$\int \tilde{G}^2(\xi, \boldsymbol{\rho})\, d^2\boldsymbol{\rho} = \frac{1}{4\pi\alpha'\xi} \cdot \left(\frac{1}{2}\right) \int \frac{\mathrm{e}^{-2\cdot\boldsymbol{\rho}^2/4\alpha'\xi}}{4\pi\alpha'\xi} \cdot 2\, d^2\boldsymbol{\rho} = \frac{1}{8\pi\alpha'\xi}. \quad (14.31)$$

The two-pomeron branching contribution falls with 'time' as $1/\xi$. What is the meaning of this smallness?

In (14.30a), a certain source produces a diffusive distribution (in our case, $\delta(\boldsymbol{\rho} - \boldsymbol{\rho}_1)$ at $\xi = 0$). With the increase of ξ, the integral over $\boldsymbol{\rho}$ of the distribution stays constant; the total probability to find a particle anywhere in space is determined solely by the power of the source and does not depend on time.

In (14.30a) we create two diffusion waves (with N their emission amplitude). If at time $\xi > 0$ I measured them *independently*, the probability conservation would have been intact, as in the one-pomeron case.

However, the amplitude we are interested in is given by the probability to find the two particles *in the same point* $\boldsymbol{\rho}_2$, ξ_2. Such probability is inversely proportional to the typical area the distribution spreads over in time ξ, that is $1/\langle \boldsymbol{\rho}^2 \rangle \sim 1/\alpha'\xi$.

Investigating the flow coming from the centre, at large distances a single particle (**P**) gives the leading contribution $\propto \exp(-\boldsymbol{\rho}^2/4\alpha'\xi)$. The corrections (**PP**) fall faster with the distance, $\propto \exp(-2 \cdot \boldsymbol{\rho}^2/4\alpha'\xi)$, although they may be significant at large times (and finite $\boldsymbol{\rho}^2$). Such an interpretation looks quite satisfactory. Recall, however, how the same situation looked in the momentum representation:

$$G^{(\mathbf{P})}(\xi, \mathbf{k}^2) \sim \exp\big(-\alpha'\xi\mathbf{k}^2\big), \qquad G^{(\mathbf{PP})}(\xi, \mathbf{k}^2) \sim \exp\big(-\tfrac{1}{2} \cdot \alpha'\xi\mathbf{k}^2\big).$$

Now, when ξ is large, the second contribution is larger than the first one! The picture in the impact parameter space turned out to be intuitively more satisfactory than that in the momentum representation.

Similarly, we can 'spell out' any diagram in the language of diffusion. For example, the enhanced graph shown in (14.32) corresponds to the creation of one particle at the impact parameter point $\boldsymbol{\rho}_1$ at time ξ_1, which splits into two particles at $\boldsymbol{\rho}_2$, ξ_2. These particles then combine at a space–time point $\boldsymbol{\rho}_3$, ξ_3 into one, which one is then registered at time ξ_4 in $\boldsymbol{\rho}_4$.

$$\text{(14.32)}$$
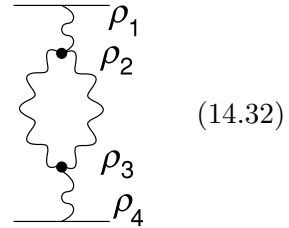
14.5.2 Energy dependence of σ_{tot}

We are ready to make an important general statement about the energy behaviour of σ_{tot}.

Consider the weak coupling regime and collect all relevant leading corrections:

$$f \simeq \quad - \quad + \quad - \quad - \quad + \quad .$$
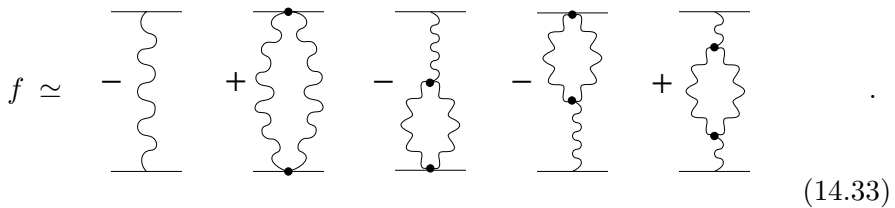
$$\text{(14.33)}$$

Let us examine the semi-enhanced diagram. Taking $\mathbf{k} = 0$ and using the expression (14.27) for the three-pomeron weak coupling vertex, for the third graph on the r.h.s. of (14.33) we have

$$g \cdot \frac{1}{\omega} \cdot \int \frac{d^2\mathbf{k}_1 \, d\omega_1}{(2\pi)^3 i} \frac{a\omega + 2 \cdot b\mathbf{k}_1^2}{(\omega_1 + \alpha'\mathbf{k}_1^2)(\omega - \omega_1 + \alpha'\mathbf{k}_1^2)} \cdot N \sim \ln\omega. \quad \text{(14.34)}$$

But if we take the Fourier transform of $\ln\omega$,

$$\int \frac{d\omega}{2\pi i} \, \mathrm{e}^{\omega\xi} \ln\omega \;\rightarrow\; \int_{-\infty}^{0} \mathrm{e}^{\omega\xi} \, d\omega \;\rightarrow\; \frac{1}{\xi},$$

we get the same $1/\xi$ behaviour as we had for the **PP** branching above. We see that the **P** pole $1/\omega$ in (14.34) has cancelled, and the contribution of the semi-enhanced diagram reduced to that of the non-enhanced one:
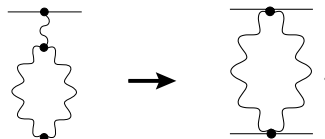
Analogous cancellation of both **P** poles occurs also in the enhanced diagram (14.32) **P** → **PP** → **P**, the last term in (14.33). There is, however, a subtle point, namely the signs. Assembling all contributions to the r.h.s. of (14.33), for the total cross section we derive

$$\sigma_{\text{tot}} = g^2 - \frac{(N - g \cdot c)^2}{8\alpha'\xi}, \qquad (14.35)$$

where we denoted by c the constant that emerges from the **P** → **PP** vertex in (14.34). This shows that if the cross section tends to a constant, then it approaches this limit *from below*.

In the strong coupling case we do not need to calculate anything, since we know already that the cross section grows logarithmically with s.

We may thus conclude that at sufficiently high energies the total cross sections *should slowly grow* with s, at least temporarily (weak coupling), if not forever (strong coupling).

14.5.3 Experimental situation

What is the experimental situation?

Up to $s \sim 30\,\text{GeV}^2$ all the cross sections decrease (but for σ_{tot}^{pp} and $\sigma_{\text{tot}}^{K^+p}$ that stay nearly constant) (Fig. 14.3). Between 70 and 2000 GeV^2 a new phenomenon takes place: the cross sections flatten off and start to slowly increase.* The fact that σ_{tot}^{pp} has a minimum, means that there exists a definite energy at which the matter is maximally transparent.

For the first time the 'complication' of the theory reveals itself; without branchings nothing of this kind would happen.

14.5.4 Would one ever reach the true asymptotics?

An impressive body of predictions of the theory has been experimentally confirmed. Among them are the following statements.

(1) Factorization of scattering amplitudes and cross sections.

(2) Universal nature of particle production in the plateau region.

(3) High-mass inelastic diffraction in the three-pomeron limit, whose mass distribution is spectacularly different from expectations based on the statistical model of the hadron production.

(4) Shrinkage of the diffractive cone.

---

* From the RFT perspective, growing total cross sections (Fig. 14.3) may shift ones preference towards the strong coupling regime (ed.).
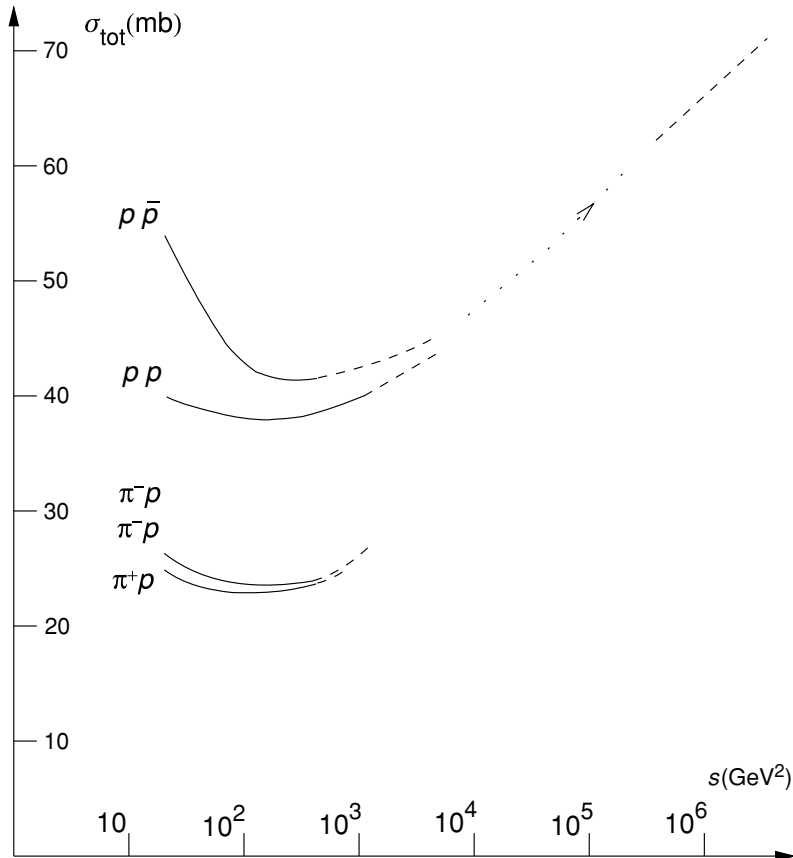
Fig. 14.3   Sketch of the total hadron cross sections $\sigma_{\text{tot}}(s)$. Hadron accelerator data that appeared after middle-1970s are shown by dashed lines.

(5) Increase of the total cross sections with $\ln s$, which signals either an approach to asymptotic constant values (weak coupling) or a steady growth characteristic of the strong coupling regime.

Many attempts were made to describe also the *angular distributions*. Qualitatively, it has become apparent that the branchings play an essential rôle here. At the same time, quantitative description of the t-dependence has not been achieved.

At first sight, the procedure seems well defined and simple; one has to substitute known expressions into given formulae, calculate the effect and compare the prediction with the data. Strangely enough (accidentally or, may be, for a deep reason beyond our understanding) this happens to be an impossible task.

We assume ξ to be large. The true parameter of the problem is, however, $\alpha'\xi$. The easiest way to see this is by recalling the two-pomeron branching,

$$= \tilde{G}^2(\xi, \boldsymbol{\rho}_1 - \boldsymbol{\rho}_2)N^2. \qquad (14.36)$$

Dealing with this diagram, a number is substituted for the reggeon emission amplitude N. My motivation was that I am close to the singularity in ω. If so, ξ is large, and so is, consequently, the transverse distance $|\boldsymbol{\rho}_1 - \boldsymbol{\rho}_2|$ due to diffusive nature of the pomeron, $G \sim \exp(-|\Delta\boldsymbol{\rho}|^2/4\alpha'\xi)$.

In fact, the hadron projectile has its own transverse size R, so that inside the vertex part N there are various diagrams in which impact parameters of participating particles vary within $|\Delta\boldsymbol{\rho}| \lesssim R$. Therefore we should have introduced separate transverse coordinates for the reggeons and should have written a multiple integral over the impact parameters,

$$\sim \int N(\boldsymbol{\rho}_1; \boldsymbol{\rho}_1', \boldsymbol{\rho}_1'')\tilde{G}(\xi, \boldsymbol{\rho}_1' - \boldsymbol{\rho}_2')\tilde{G}(\xi, \boldsymbol{\rho}_1'' - \boldsymbol{\rho}_2'')N(\boldsymbol{\rho}_2; \boldsymbol{\rho}_2', \boldsymbol{\rho}_2'').$$

From the point of view of an asymptotic behaviour, we have acted correctly by treating N as a constant. This is, however, justified only if $R^2 \ll 4\alpha'\xi$ so that $|\boldsymbol{\rho}_1 - \boldsymbol{\rho}_2| \gg |\boldsymbol{\rho}_1 - \boldsymbol{\rho}_1'| \sim R$. And just here lies the catastrophe.

Strictly speaking, it is difficult to estimate the radius of a hadron; I would say that $R \sim 1/2m_\pi$. At the same time, the value of α' is measured from the shrinkage of the diffractive cone. It turns out to be rather small, $\alpha' \approx 1/4m_N^2$, about four times smaller than the slopes of non-vacuum Regge trajectories, $\alpha'_{\mathbf{R}} \simeq 1\,\mathrm{GeV}^{-2}$. Hence, our inequality becomes

$$4\alpha'\xi \gg R^2 \quad \Longrightarrow \quad \xi \gg \xi_{\mathrm{crit}} \equiv \frac{R^2}{4\,\alpha'} \sim \frac{m_N^2}{4m_\pi^2} \simeq 10.$$

Obviously, the condition $\xi \gg \xi_{\mathrm{crit}}$ can by no means be satisfied, ever. At best we may reach $\xi \sim \xi_{\mathrm{crit}}$ ($s = 2.000\,\mathrm{GeV}^2$ corresponds to $\xi \approx 8$).

For reasons we do not understand, there is no way to reach the true asymptotic regime.

Examining the parameters in the strong coupling regime, the situation is even worse: the corresponding diffusion coefficient (effective α') turns out to be even smaller.

The appearance of a new small parameter, $1/\xi_{\mathrm{crit}} = 4\alpha'/R^2 \ll 1$, on the other hand, suggests certain simplifications for the region of moderately high energies, $\xi \lesssim \xi_{\mathrm{crit}}$. Since in the $\alpha' \to 0$ limit the impact parameter diffusion disappears and parallel showers do not separate but keep interacting with each other; employing α' as a small parameter leads to a picture of 'heavy pomeron', whose image is no longer a two-particle 'ladder' but a more complicated t-channel state of many re-interacting particles (Gribov, 1976).

To conclude, our object diffuses in unit time at a typical transverse distance $|\Delta\boldsymbol{\rho}|^2 \sim 4\alpha'$ (the diffusion coefficient). Why did this distance turn out to be *much smaller* than the size proper of the hadron? Qualitatively, this phenomenon may be due to the fact that hadrons are *composite*. If the true fundamental objects – quarks – are more compact, their smaller size would introduce a relatively large mass scale parameter that might explain the smallness of the slope α' of the t-channel vacuum exchange.

It is just the smallness of α' which impairs quantitative description of the t-dependence of hadron–hadron scattering amplitudes. There is, however, a whole complex of problems not related to the angular distributions, like multi-particle production processes, and it is necessary to understand the physics which corresponds to them.